Multipole decomposition of the rate of muon-to-electron ($\mu^- \longrightarrow e^-$) conversion in ^{208}Pb

O. Civitarese[1,2,*] and T. Tarutina[2]
[1]*Department of Physics, University of La Plata, C.C. 67 1900, La Plata, Argentina*
[2]*IFLP (CONICET) La Plata, Argentina*

(Received 6 November 2018; revised manuscript received 8 May 2019; published 28 June 2019)

The ($\mu^- \longrightarrow e^-$) conversion in ^{208}Pb nucleus is studied. For the elementary process we consider the most general effective Lagrangian responsible for the lepton-flavor violation. For the nuclear structure part, the spectrum of ^{208}Pb is calculated by performing a diagonalization of the δ-force interaction in the space of particle-hole pairs for neutrons and protons. We calculate the coherent contribution by direct summation of single-particle excitations. The noncoherent muon-to-electron conversion is calculated by summing over the contributions for all possible intermediate states in ^{208}Pb. We perform the multipole decomposition of the transition amplitude and present the nuclear matrix elements of spin-dependent and spin-independent operators appearing in the total rate of the muon to electron conversion process. The results are presented in a way to facilitate their use in model building of the electroweak process.

DOI: 10.1103/PhysRevC.99.065504

I. INTRODUCTION

The muon-to-electron conversion in the presence of atomic nuclei is one of the lepton-flavor-violation (LFV) processes that has attracted quite a lot of interest both theoretically and experimentally (see, for example, Refs. [1,2] and references therein). This process cannot be described in the framework of the standard model (SM) of electroweak interactions and its experimental detection would be an indication of new physics beyond the SM.

For the sake of completeness we shall briefly review the current status of the ($\mu^- \longrightarrow e^-$) conversion. From the experimental point of view several upper limits to the decay rate have been established by the SINDRUM-II experiment [3], at the level of 10^{-13} for the branching ratios $R_{\mu e}$=Γ($\mu^- \longrightarrow e^-$ conversion)/Γ(muon capture). Future experiments aim at sensitivities of the order of 10^{-17} or similar (Mu2e at Fermilab [4] and COMET at J-PARC [5]).

From the theoretical point of view, the calculations of the $R_{\mu e}$ rates focused on the particle-physics aspects of the problem [6–9], on the extensions of the SM to accommodate for lepton-flavor violation [10,11], and, more recently, on the nuclear structure aspects related to the calculations of n-order matrix elements of operators in ($\mu^- \longrightarrow e^-$) process [12–19].

Among the theoretical works, Ref. [20] presents a complete analysis of the electroweak channels which become operative if lepton-flavor violation is allowed. The effective Lagrangian of Ref. [20] describes the ($\mu^- \longrightarrow e^-$) at the quark level and then, by introducing suitable form factors, the authors of Ref. [20] have obtained an effective Lagrangian at the nucleon level. Nuclear correlations, in the coherent channel of ($\mu^- \longrightarrow e^-$), are taken into account in Ref. [20] by introducing nuclear matter and charge density distributions. Therefore this Lagrangian becomes a good starting point for the calculation of currents in finite nuclei.

In this paper we study muon to electron conversion in the presence of ^{208}Pb. We are interested here in the comparative estimation of spin-dependent and spin-independent contributions to the nuclear response [21–24]. We consider a Lagrangian like the one proposed in Ref. [20] and for the nuclear structure part we diagonalize a δ-force interaction to calculate the spectrum of ^{208}Pb, as done in Ref. [25] for the calculation of the cross section for the neutrino-nucleus scattering ^{208}Pb(g.s.)(ν, ν')^{208}Pb.

In order to facilitate new theoretical analysis of ($\mu^- \longrightarrow e^-$) conversion we have, separately, presented the nuclear components of the decay rate, e.g., both by the tensorial structure of the participant operators as well as for the proton and neutron components of the nuclear wave functions.

As done recently in Ref. [19], different models where ($\mu^- \longrightarrow e^-$) can take place enter the calculation through combinations of coefficients which stem from the properties of the mediators, e.g., Z_0 and W bosons, as well as super symmetric (SUSY) particles [19], in models beyond the SM. As shown in Ref. [20] there are more possibilities when the Lagrangian is written at the very elementary level of four fermion interactions. Therefore, these models may become manageable provided the nuclear structure part is given independently of the adopted particle-physics model. More specifically, from the nuclear structure part of the problem, the extent of the spin dependence of the calculated nuclear matrix elements becomes relevant for experimental reasons [26].

The paper is organized as follows: The formalism is described in Sec. II, where the details of the LFV Lagrangian are given (Sec. II A), together with the nuclear structure part of the formalism (Sec. II B). The results of the calculations are presented and discussed in Sec. III. Finally, our conclusions are drawn in Sec. IV.

*osvaldo.civitarese@fisica.unlp.edu.ar

II. FORMALISM

Anomalous muon-to-electron conversion is a process where, in the presence of an atomic nucleus, a negative muon transforms into an electron without emitting a neutrino [27]:

$$\mu^- + (A, Z) \longrightarrow e^- + (A, Z)^*. \tag{1}$$

In such a process the lepton-flavor numbers L_e and L_μ are not conserved while the total lepton number is conserved.

The emitted electron has a momentum given by

$$|p_e| = m_\mu - \epsilon_b - (E_f - E_i), \tag{2}$$

where m_μ is the mass of muon, ϵ_b is the muon binding energy in the $1s$ state of the muonic atom, and $E_i(E_f)$ are the energies of the initial (final) states of the nucleus.

Below we will consider the coherent and noncoherent muon conversion processes. In the former, the final state of the nucleus is its ground state, while in the latter the nucleus is left in an excited state. The coherent process is characterized by the largest value of the momentum of the emitted electron.

The probability of muon-to-electron conversion process in nuclei is given Ref. [11], and it reads

$$\Gamma_{i\to f} = \frac{2\pi}{\hbar}\int d\hat{\mathbf{p}}_e \left(\frac{p_e}{m_\mu}\right)^2 |\langle f|\Omega|i,\mu\rangle|^2 \ \Xi, \tag{3}$$

where $\langle f|\Omega|i,\mu\rangle$ is the matrix element of the operators involved in the process between the initial (i) and final (f) nuclear states, $\mathbf{p}_e$ is the momentum of the emitted electron, and Ξ depends on the specific model adopted to describe the elementary LFV process.

A. The effective Lagrangian

The most general effective LFV Lagrangian in the nonphotonic sector and at the quark-lepton level can be written in the form:

$$\begin{aligned}\mathcal{L}_{np} = &-\frac{G_F}{\sqrt{2}}\sum_{q=u,d,s,..}\Big\{[g_{LS}(q)\bar{e}_L\mu_R + g_{RS}(q)\bar{e}_R\mu_L]\bar{q}q + [g_{LP}(q)\bar{e}_L\gamma_5\mu_R + g_{RP}(q)\bar{e}_R\gamma_5\mu_L]\bar{q}\gamma_5 q\\ &+ [g_{LV}(q)\bar{e}_L\gamma^\mu\mu_R + g_{RV}(q)\bar{e}_R\gamma^\mu\mu_L]\bar{q}\gamma_\mu q + [g_{LA}(q)\bar{e}_L\gamma^\mu\gamma_5\mu_L + g_{RA}(q)\bar{e}_R\gamma^\mu\gamma_5\mu_R]\bar{q}\gamma_\mu\gamma_5 q\\ &+ \tfrac{1}{2}[g_{LT}(q)\bar{e}_L\sigma^{\mu\nu}\mu_R + g_{RT}(q)\bar{e}_R\sigma^{\mu\nu}\mu_L]\bar{q}\sigma_{\mu\nu}q\Big\}\\ = &\,\mathcal{L}_S + \mathcal{L}_P + \mathcal{L}_V + \mathcal{L}_A + \mathcal{L}_T,\end{aligned} \tag{4}$$

where G_F is the Fermi constant and $g_{XK}(q)$ are dimensionless coupling constants at the quark level (q) with $X = \{L, R\}$ (left or right) and $K = \{S, P, V, A, T\}$ (for scalar, pseudo-scalar, vector, axial-vector, and tensor terms, respectively). $e_{L(R)}$ and $\mu_{L(R)}$ are the electron and muon left (right) fields, defined by the action of the projectors $P_L = (1-\gamma_5)/2$ and $P_R = (1+\gamma_5)/2$, $\sigma_{\mu\nu} = (i/2)[\gamma_\mu, \gamma_\nu]$, and γ_μ are Dirac's matrices. The value of the four-fermion coupling constants can be calculated using specific models of the LFV process. Some of these models are, for example, the W exchange [28], supersymmetric theories [28], SUSY models with R-parity breaking [29], tree diagrams involving Z' [30], etc.

The Lagrangian of Eq. (4) can be rewritten using the isospin formalism at the nucleonic level and reads as follows:

$$\begin{aligned}\mathcal{L}_{np} = &-\frac{G_F}{\sqrt{2}}\big(\bar{e}_L\mu_R\overline{\psi}\big[g^{(0)}_{LS} + g^{(1)}_{LS}\tau_3\big]\psi + \bar{e}_R\mu_L\overline{\psi}\big[g^{(0)}_{RS} + g^{(1)}_{RS}\tau_3\big]\psi + \bar{e}_L\gamma^5\mu_R\overline{\psi}\gamma_5\big[g^{(0)}_{LP} + g^{(1)}_{LP}\tau_3\big]\psi + \bar{e}_R\gamma^5\mu_L\overline{\psi}\gamma_5\big[g^{(0)}_{RP} + g^{(1)}_{RP}\tau_3\big]\psi\\ &+ \bar{e}_L\gamma^\mu\mu_L\overline{\psi}\gamma_\mu\big[g^{(0)}_{LV} + g^{(1)}_{LV}\tau_3\big]\psi + \bar{e}_R\gamma^\mu\mu_R\overline{\psi}\gamma_\mu\big[g^{(0)}_{RV} + g^{(1)}_{RV}\tau_3\big]\psi + \bar{e}_L\gamma^\mu\gamma^5\mu_L\overline{\psi}\gamma_\mu\gamma_5\big[g^{(0)}_{LA} + g^{(1)}_{LA}\tau_3\big]\psi\\ &+ \bar{e}_R\gamma^\mu\gamma^5\mu_R\overline{\psi}\gamma_\mu\gamma_5\big[g^{(0)}_{RA} + g^{(1)}_{RA}\tau_3\big]\psi + \tfrac{1}{2}\big\{\bar{e}_L\sigma^{\mu\nu}\mu_L\overline{\psi}\sigma_{\mu\nu}\big[g^{(0)}_{LT} + g^{(1)}_{LT}\tau_3\big]\psi + \bar{e}_R\sigma^{\mu\nu}\mu_R\overline{\psi}\sigma_{\mu\nu}\big[g^{(0)}_{RT} + g^{(1)}_{RT}\tau_3\big]\psi\big\}\big),\end{aligned} \tag{5}$$

where $\psi = (p, n)^T$ and $g^{(0)}_{XK}$ and $g^{(1)}_{XK}$ are isoscalar and isovector coupling constants. These constants are connected with coupling constants at the quark level through:

$$\begin{aligned}g^{(0)}_{XK} &= \frac{1}{2}\sum_{q=u,d,s}\big[g_{XK}(q)G^{(q,p)}_K + g_{XK}(q)G^{(q,n)}_K\big]\\ g^{(1)}_{XK} &= \frac{1}{2}\sum_{q=u,d,s}\big[g_{XK}(q)G^{(q,p)}_K - g_{XK}(q)G^{(q,n)}_K\big],\end{aligned} \tag{6}$$

where $G^{(q,p)}_K$ are form factors (see Ref. [18] and references therein) obeying the relations

$$G^{(u,p)}_K = G^{(d,n)}_K, \quad G^{(d,p)}_K = G^{(u,n)}_K, \quad G^{(s,p)}_K = G^{(s,n)}_K, \tag{7}$$

where u, d, and s are quark indices and p and n stand for protons and neutrons, respectively. These form factors are presented in Table I, and their values have been obtained under the conditions of isospin invariance. Below we define the coupling constants for neutron $g_{XK}(n)$ and proton $g_{XK}(p)$ states which are related with the above $g^{(0)}_{XK}$ and $g^{(1)}_{XK}$ by:

$$\begin{aligned}g_{XK}(n) &= g^{(0)}_{XK} - g^{(1)}_{XK}\\ g_{XK}(p) &= g^{(0)}_{XK} + g^{(1)}_{XK}.\end{aligned} \tag{8}$$

TABLE I. Values of the form factors from Eq. (6), as given in Ref. [18].

$G_V^{(u,p)} = 2$	$G_V^{(d,p)} = 1$	$G_V^{(s,p)} = 0$
$G_A^{(u,p)} = 0.78$	$G_A^{(d,p)} = -0.47$	$G_A^{(s,p)} = -0.19$
$G_S^{(u,p)} = 5.1$	$G_S^{(d,p)} = 4.3$	$G_S^{(s,p)} = 2.5$
$G_P^{(u,p)} = 103$	$G_P^{(d,p)} = 100$	$G_P^{(s,p)} = 3.3$

B. Relevant operators and nuclear matrix elements

In order to use the Lagrangian in Eq. (5), in conjunction with a nonrelativistic description of the nucleus, one needs to reduce the operators in Eq. (5) to their nonrelativistic limit. This is performed using Foldy-Wouthuysen transformation [31] and various operators appear that are similar to those of the standard β-decay theory as given, for example, in Ref. [32].

To quantify the rate of $(\mu^- \longrightarrow e^-)$ conversion that leaves the nucleus in some final state $|J_f M_f\rangle$ we calculate the expectation values of the Lagrangian between the initial $|i\rangle$ and final $|f\rangle$ states $\langle f|\mathcal{L}|i\rangle$, where in the present case, taking ^{208}Pb as the host nucleus, they are written as follows:

$$\begin{aligned} |i\rangle &= |^{208}\text{Pb, gs}\rangle \otimes |\mu^-, \text{bound}\rangle \\ |f\rangle &= |^{208}\text{Pb, exc} + \text{gs}\rangle \otimes |e^-, \text{outgoing}\rangle, \end{aligned} \tag{9}$$

averaged over the spin of the initial state of the nucleus and of the muon and summed over the final states of the nucleus and of the outgoing electron.

The wave function, $|JM, k\rangle$ of the excited kth state in ^{208}Pb is constructed as a superposition of neutron particle-hole states $|nn'^{-1}; JM\rangle$ and proton particle-hole states $|pp'^{-1}; JM\rangle$ which we can write in a compact way suitable for later use, namely:

$$|JM, k\rangle = \sum_{\rho\equiv(nn'^{-1}),(pp'^{-1})} C^{(k)}(\rho)|\rho; JM\rangle. \tag{10}$$

The quantities $C^{(k)}(\rho)$ with $\rho \equiv \{(nn'^{-1}), (pp'^{-1})\}$ are the amplitudes obtained by a direct diagonalization of the residual two-body interaction, which in this work is the δ-force interaction of Ref. [33].

To obtain the expression for M_{Nucl} the effective interaction is expanded in powers of the inverse nucleon mass M_N^{-1} and in the limit of small momenta, $p_N/M_N \ll 1$, where p_N is the momentum of the nucleon, one obtains:

$$M^2_{\text{Nucl}}\left(J^\pi_f\right) = M^2(\langle \mathbf{1}\rangle) + M^2(\langle \sigma\rangle) + M^2(\Lambda), \tag{11}$$

where the quantities $M^2(\langle \mathbf{1}\rangle)$, $M^2(\langle \sigma\rangle)$, and $M^2(\Lambda)$ are the spin-independent, spin-dependent, and tensor parts, respectively, of the squared matrix element.

For the spin-independent part we write

$$M^2(\langle \mathbf{1}\rangle) = m_e c_1 + E_e c_2 - \frac{1}{2M_N} p_e^2 c_3, \tag{12}$$

where m_e, p_e, and E_e are the mass, momentum, and energy of the emitted electron. The coefficients c_1, c_2, and c_3 in Eq. (12) are given by

$$\begin{aligned} c_1 &= \sum_{qq'=(p,n)} \{2g_{LS}(q)g_{RS}(q') + 2g_{LS}(q)g_{RV}(q') + 2g_{RV}(q)g_{LV}(q') + g_{RS}(q)g_{LV}(q') + g_{RS}(q)g_{RV}(q')\}\mathcal{M}(qq', l\ \gamma = 0\ J) \\ c_2 &= \sum_{qq'=(p,n)} \{2g_{LS}(q)g_{LV}(q') + 2g_{RS}(q)g_{RV}(q') + 2g_{RV}(q)g_{RV}(q') + g_{LS}(q)g_{LS}(q') + g_{RS}(q)g_{RS}(q')\}\mathcal{M}(qq', l\ \gamma = 0\ J) \\ c_3 &= \sum_{qq'=(p,n)} \{g_{LS}(q)g_{LV}(q') + g_{RS}(q)g_{RV}(q') - g_{LS}(q)g_{LT}(q') - g_{RS}(q)g_{RT}(q') + g_{RV}(q)g_{RV}(q') + g_{LV}(q)g_{LV}(q') \\ &\quad - g_{RV}(q)g_{RT}(q') - g_{LV}(q)g_{LV}(q')\}\mathcal{M}(qq', l\ \gamma = 0\ J), \end{aligned} \tag{13}$$

where the summations are performed on neutron ($q = n$) and proton($q = p$) states and the nuclear matrix elements are defined by

$$\mathcal{M}(qq', l\ \gamma = 0\ J) = \sum_{k,k',\rho,\rho'} C^{(k)}(\rho)C^{(k')*}(\rho')\langle \rho, k||T^{(l,0)J}||0^+\rangle\langle \rho', k'||T^{(l,0)J}||0^+\rangle^*. \tag{14}$$

The operator $T^{(l,0)J}$ is defined as follows:

$$T^{(l,0)JM} = \delta_{lJ}\sqrt{4\pi} i^l j_l(p_e r) g(r) Y_{lM}(\hat{\mathbf{r}}), \tag{15}$$

where $g(r)$ is the radial wave function of the muon in the $1s$ state of the muonic atom.

For the spin-dependent part we write

$$M^2(\langle \sigma\rangle)) = m_e c_1' + E_e c_2' - \frac{1}{2M_N} p_e^2 c_3', \tag{16}$$

where the coefficients c_1', c_2', and c_3' are given by

$$c_1' = \sum_{qq'=(p,n)} \{2g_{RA}(q)g_{LA}(q') + 2g_{RA}(q)g_{LT}(q') + 2g_{LA}(q)g_{RT}(q') + 2g_{LT}(q)g_{RT}(q')\}\mathcal{M}(qq', l\ \gamma = 1\ J)$$

$$c_2' = \sum_{qq'=(p,n)} \{2g_{RA}(q)g_{RT}(q') + 2g_{LA}(q)g_{LT}(q') + g_{RA}(q)g_{RA}(q') + g_{LA}(q)g_{LA}(q') + g_{LT}(q)g_{LT}(q') + g_{RT}(q)g_{RT}(q')\}\mathcal{M}(qq', l\ \gamma = 1\ J)$$

$$c_3' = \sum_{qq'=(p,n)} \{2[-g_{LP}(q)g_{LA}(q') - g_{RP}(q)g_{RA}(q') - g_{LP}(q)g_{LT}(q') - g_{RP}(q)g_{RT}(q') + g_{RA}(q)g_{RA}(q') + g_{LA}(q)g_{LA}(q') - g_{RA}(q)g_{RT}(q') - g_{LA}(q)g_{LT}(q')]\}\mathcal{M}(qq', l\ \gamma = 1\ J), \tag{17}$$

and

$$\mathcal{M}(qq', l\ \gamma = 1\ J) = \sum_{k,k',\rho,\rho'} C^{(k)}(\rho)C^{(k')*}(\rho')\langle\rho, k||T^{(l,1)J}||0^+\rangle\langle\rho', k'||T^{(l,1)J}||0^+\rangle^*. \tag{18}$$

The spin-dependent operator $T^{(l,1)J}$ is defined as follows:

$$T^{(l,1)JM} = \sqrt{4\pi}i^l j_l(p_e r)g(r)[Y_l(\hat{\mathbf{r}}) \times \sigma]^{(JM)}. \tag{19}$$

Finally, the tensor part is written

$$M^2(\Lambda) = -\frac{1}{2M_N}p_e^2\sqrt{\frac{2}{3}}c_3'', \tag{20}$$

where the coefficient c_3'' is given by

$$c_3'' = \sum_{qq'=(p,n)} \{[-2g_{LP}(q)g_{LA}(q') - 2g_{RP}(q)g_{RA}(q') - 2g_{LP}(q)g_{LT}(q') - 2g_{RP}(q)g_{RT}(q') + g_{RA}(q)g_{RA}(q') + g_{LA}(q)g_{LA}(q') - g_{LT}(q)g_{LT}(q') - g_{RT}(q)g_{RT}(q')]\}\mathcal{M}(qq'), \tag{21}$$

and the nuclear matrix elements read

$$\mathcal{M}(qq') = \sum_{kk',\rho,\rho'} C^{(k)}(\rho)C^{(k')*}(\rho')\left(\frac{5}{6}\right)^2\frac{4\pi}{2J_i+1}\sum_{l,l',K}(-1)^{l/2-l'/2+K}\sqrt{(2l+1)(2l'+1)}\begin{pmatrix} l & l' & 2 \\ 0 & 0 & 0\end{pmatrix}\begin{Bmatrix} 1 & 1 & 2 \\ l' & l & K\end{Bmatrix} \times \langle\rho, k||i^l j_l(p_e r)g(r)[Y_l(\hat{\mathbf{r}}) \times \sigma]^{(K)}||0^+\rangle\langle\rho', k'||i^{l'} j_{l'}'(p_e r)g(r)[Y_{l'}(\hat{\mathbf{r}}) \times \sigma]^{(K)}||0^+\rangle^*. \tag{22}$$

In the above equations, we have adopted the notation and the phase convention given in Ref. [34], concerning the matrix elements of tensor operators written in spherical coordinates and spherical single-particle states. In Eqs. (15), (19), and (22), the operators $T^{(l,\gamma)JM}$ are acting on single nucleon coordinates, which have been omitted for simplicity.

C. Coherent and noncoherent transitions

The noncoherent part of the probability $\Gamma_{i\to f}$ of Eq. (3) is then calculated by taken the matrix elements of the transition operators between the ground state and excited states of the nuclear spectrum. Using the square matrix elements of Eq. (11) one obtains:

$$M^2_{\text{gs}\longrightarrow\text{exc}} = \sum_f \left(\frac{p_{e_f}}{m_\mu}\right)^2 M^2_{\text{Nucl}}(J_f^\pi), \tag{23}$$

where "gs" denotes the ground state of the nucleus and the subindex "f" stands for the final excited nuclear state.

The coherent part of the transition is calculated from the expectation value of the spin-independent operator $j_0(p_e r)$ in the ground state of the nucleus. It is clear that, from the effective Lagrangian given by Eq. (5), only the scalar and vector terms will contribute to the squared matrix element of the coherent process. Using the notation of Ref. [13] the squared matrix element can be written:

$$M^2_{\text{gs}\longrightarrow\text{gs}} = (3g_V f_V)^2\left[\left(1+\tfrac{1}{3}\beta\right)ZF_Z + \left(1-\tfrac{1}{3}\beta\right)NF_N\right]^2, \tag{24}$$

with the proton and neutron nuclear form factors F_Z and F_N given by the expressions

$$F_Z = \frac{1}{Z}\sum_j (2j+1)\langle j||j_0(|\mathbf{p_e}|r)||j\rangle\left(V_j^Z\right)^2$$

$$F_N = \frac{1}{N}\sum_j (2j+1)\langle j||j_0(|\mathbf{p_e}|r)||j\rangle\left(V_j^N\right)^2, \tag{25}$$

where V_j^Z and V_j^N are the occupation factors for proton and neutron single-particle states. In our model, $V_j^Z(V_j^N) = 1(0)$ for occupied (empty) single-particle states since we are dealing with a double-close shell nuclei. The quantities g_V, f_V, and β depend on the particular gauge model responsible for the elementary muon to electron conversion. The advantage

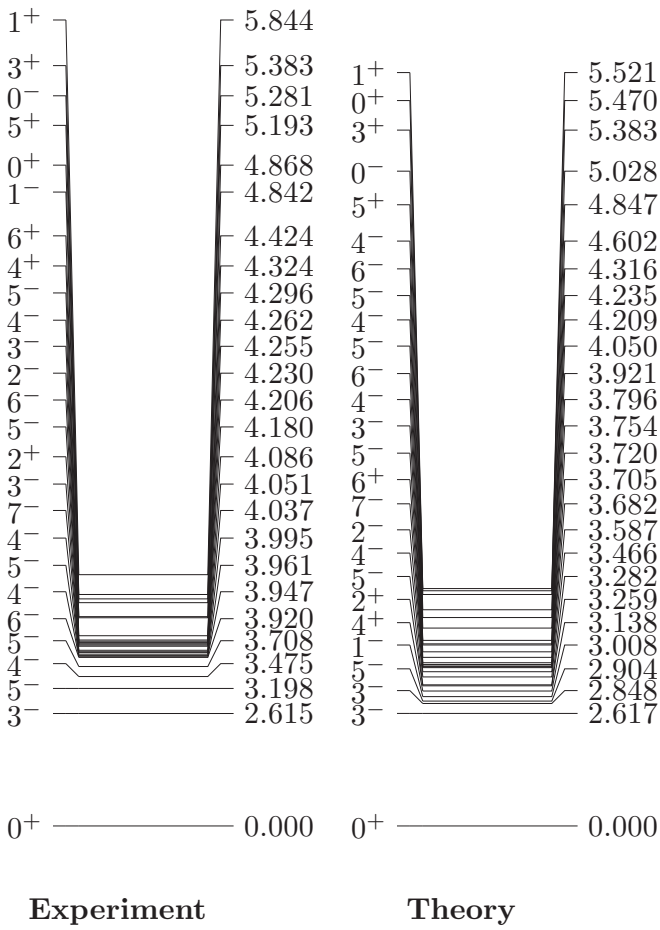

FIG. 1. Calculated and experimental energy levels of ^{208}Pb. The results have been obtained by diagonalizing the delta force interaction in the space of particle-hole configurations in a basis of single-particle states up to three mayor shells around the neutron and protons shell closures $N = 126$ and $Z = 82$. All values are given in units of MeV. The parameters used in the calculations are given in Refs. [25,35]. The experimental data are taken from Ref. [37].

of using the form factors F_Z and F_N is that they depend only on the nuclear structure quantities and are independent of the specific model of the LFV process.

III. RESULTS AND DISCUSSIONS

A. Nuclear structure of ^{208}Pb

The single-particle neutron and proton states, which are included in the single-particle basis, are the harmonic oscillator states listed in Table I of Ref. [25]. The values of these single-particle energies were taken from Refs. [35,36] and several of them were adjusted to reproduce the observed single-particle energies and spin sequences in the region of $A = 208$. To obtain the wave functions of the excited states of ^{208}Pb we have diagonalized the δ-force interaction, with parameters adjusted to reproduce the energy of the first excited $J^\pi = 3^-$ state in ^{208}Pb. A detailed comparison between experimental and calculated energy spectra and transition probabilities have been presented in Ref. [25] and it will be omitted here for brevity. For the sake of completeness we present in Fig. 1 the lowest portion of the calculated and experimental energy levels of ^{208}Pb.

B. Muon and electron states

For the leptonic part we have solved the Dirac equation numerically using the parameters given in Ref. [38]. Both the large and small radial components of the muon spinor are shown in Fig. 2. The outgoing electron is taken as a plane wave. Following the discussion advanced in Ref. [20], concerning the sensitivity of the transition amplitude of the moun to electron conversion on the muon wave function, we have compared it with the normalized asymptotic form $\sin(m_\mu r)/m_\mu$ (see Fig. 2) and computed the average value of the large component of the muon spinor weighted by the proton and neutron densities [34], leading to the expressions

$$\langle g(r)\rangle_p^2 = \int_0^\infty dr 4\pi g(r)^2 \rho_p(r)$$
$$\langle g(r)\rangle_n^2 = \int_0^\infty dr 4\pi g(r)^2 \rho_n(r), \qquad (26)$$

for the average taken with proton (p) and neutron (n) densities. The results are of the order of $\langle g(r)\rangle_p^2 = 0.334$ and $\langle g(r)\rangle_n^2 = 0.496$, respectively. From these results it is seen that the calculated radial part of the muon spinor is roughly peaked at the nuclear surface and it does not have nodes except at the origin, at variance with the approximated form.

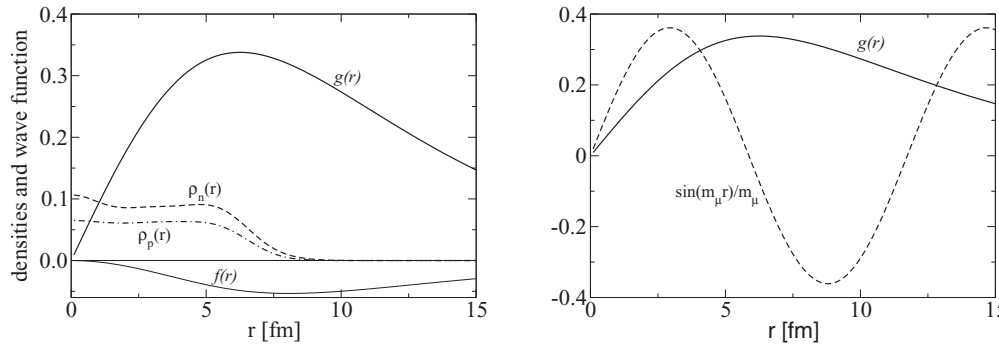

FIG. 2. Radial muon wave function and nuclear densities of ^{208}Pb. Left: Large $[g(r)]$ and small $[f(r)]$ components of the muon wave function, together with the proton and neutron densities of ^{208}Pb as a function of the radius. Right: Large component of the muon wave function $g(r)$ compared to normalized $\sin(m_\mu r)/m_\mu$.

TABLE II. Nuclear matrix elements, of the orbital, spin, and tensor operators [see Eqs. (14), (18), and (22)]. With $q = p$ or n, we indicate the structure of the particle-hole excitations, that is p means proton (particle)–proton (hole), and n means neutron (particle)–neutron (hole) configurations. With p_{e_f}, m_μ, E_{e_f}, and M_N we denote the momentum of the outgoing electron, the muon rest-mass, the outgoing electron energy and the nucleon mass, respectively. In all of these matrix elements the μ-wave function is considered as indicated in Eqs. (15), (19), and (22).

	$q, q' = p, p'$	$q, q' = n, n'$	$q, q' = p, n'$
$\sum_f (p_{e_f}/m_\mu)^2 m_e \mathcal{M}_{\langle \mathbf{1} \rangle}(qq')$	0.445×10^{-2}	0.387×10^{-2}	0.261×10^{-3}
$\sum_f (p_{e_f}/m_\mu)^2 E_{e_f} \mathcal{M}_{\langle \mathbf{1} \rangle}(qq')$	0.716	0.660	0.615×10^{-1}
$\sum_f (p_{e_f}/m_\mu)^2 p_{e_f}^2/(2M_N) \mathcal{M}_{\langle \mathbf{1} \rangle}(qq')$	0.315×10^{-1}	0.308×10^{-1}	0.360×10^{-2}
$\sum_f (p_{e_f}/m_\mu)^2 m_e \mathcal{M}_{\langle \sigma \rangle}(qq')$	0.455×10^{-2}	0.400×10^{-2}	-0.381×10^{-4}
$\sum_f (p_{e_f}/m_\mu)^2 E_{e_f} \mathcal{M}_{\langle \sigma \rangle}(qq')$	0.719	0.675	-0.116×10^{-1}
$\sum_f (p_{e_f}/m_\mu)^2 p_{e_f}^2/(2M_N) \mathcal{M}_{\langle \sigma \rangle}(qq')$	0.311×10^{-1}	0.310×10^{-1}	-0.762×10^{-3}
$\sum_f (p_{e_f}/m_\mu)^2 p_{e_f}^2/(2M_N) \mathcal{M}_{\langle \Lambda \rangle}(qq')$	-0.924×10^{-4}	0.362×10^{-4}	-0.206×10^{-3}

TABLE III. Idem as Table II, with the replacement of the radial dependence $g(r) j_l(p_e r)$ in Eqs. (15), (19), and (22) by $g(R) j_l(p_e r)$, with R the nuclear radius $R = 1.2A^{1/3}$ fm.

	$q, q' = p, p'$	$q, q' = n, n'$	$q, q' = p, n'$
$\sum_f (p_{e_f}/m_\mu)^2 m_e \mathcal{M}_{\langle \mathbf{1} \rangle}(qq')$	0.675×10^{-2}	0.593×10^{-2}	0.306×10^{-3}
$\sum_f (p_{e_f}/m_\mu)^2 E_{e_f} \mathcal{M}_{\langle \mathbf{1} \rangle}(qq')$	1.085	1.016	0.727×10^{-1}
$\sum_f (p_{e_f}/m_\mu)^2 p_{e_f}^2/(2M_N) \mathcal{M}_{\langle \mathbf{1} \rangle}(qq')$	0.475×10^{-1}	0.473×10^{-1}	0.426×10^{-2}
$\sum_f (p_{e_f}/m_\mu)^2 m_e \mathcal{M}_{\langle \sigma \rangle}(qq')$	0.680×10^{-2}	0.603×10^{-2}	-0.588×10^{-4}
$\sum_f (p_{e_f}/m_\mu)^2 E_{e_f} \mathcal{M}_{\langle \sigma \rangle}(qq')$	1.074	1.018	-0.163×10^{-1}
$\sum_f (p_{e_f}/m_\mu)^2 p_{e_f}^2/(2M_N) \mathcal{M}_{\langle \sigma \rangle}(qq')$	0.462×10^{-1}	0.468×10^{-1}	-0.103×10^{-2}
$\sum_f (p_{e_f}/m_\mu)^2 p_{e_f}^2/(2M_N) \mathcal{M}_{\langle \Lambda \rangle}(qq')$	-0.124×10^{-3}	0.176×10^{-4}	-0.213×10^{-3}

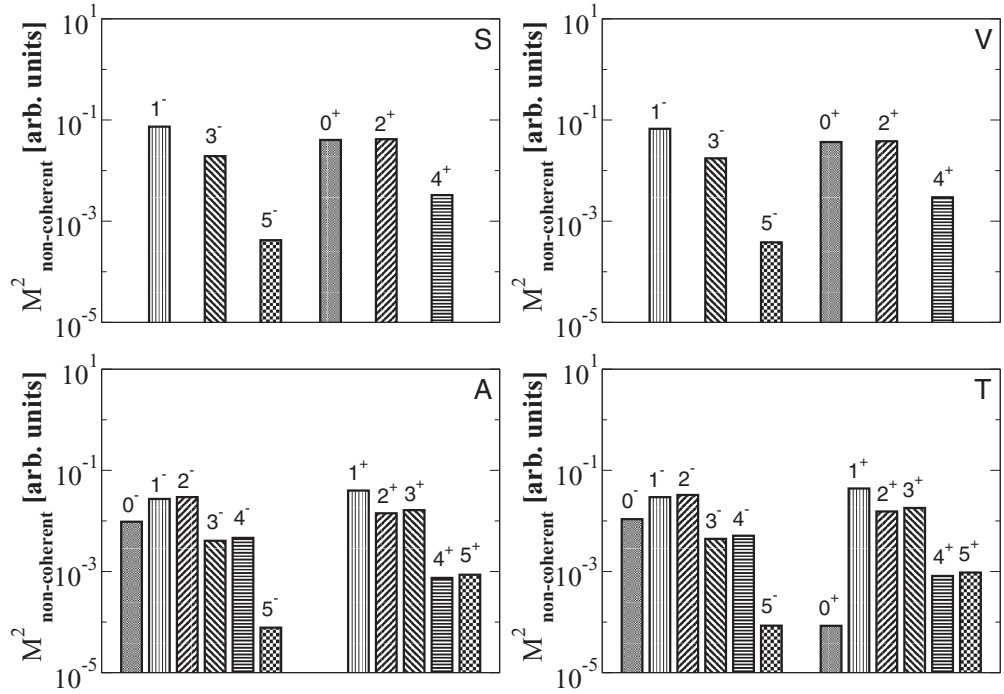

FIG. 3. Multipole decomposition of the squared matrix element of the noncoherent process for different terms of the effective Lagrangian [Eq. (5)], namely S (scalar terms), V (vector terms), A (axial-vector terms), and T (tensor terms), respectively. All values given in the figure are nuclear matrix elements square, regardless of the specific model for the ($\mu^- \longrightarrow e^-$) conversion.

TABLE IV. Contribution of different terms of the effective Lagrangian [Eq. (5)] to the total squared matrix element of the noncoherent process (second column) and its spin-independent (third column) and spin-dependent (fourth column) parts. The fifth and sixth columns show the percentages of spin-independent and spin-dependent terms to the total squared matrix element. All values are given in units of G_F^2.

Model	Total	Spin-independent Eq. (12)	Spin-dependent Eqs. (16) and (20)	Spin-independent/ total (%)	Spin-dependent/ total (%)
Scalar	2.217	2.217	0.	100	0.
Vector	2.013	2.013	0.	100	0.
Axial-vector	1.850	0.	1.850	0	100
Tensor	2.032	0.005	2.027	0.2	99.8

C. Nuclear matrix elements

In this section we consider the noncoherent part of the squared matrix element of the muon conversion in lead. The effective LFV electroweak interaction included scalar (S), vector (V), axial-vector (A), pseudo-scalar (P), and tensor (T) terms. Therefore, it is natural to begin our analysis by studying the contribution of every term of the effective Lagrangian. In this part of our work we will concentrate on the nuclear structure part of the formalism, and discuss the values of the nuclear matrix elements entering in Eqs. (23) and (24). In the later part of our analysis we will consider two specific LFV models as two possible scenarios of the process.

In this analysis we are particularly interested in determining the relative importance of the spin-dependent part of the muon-conversion probability [26]. We present below the spin-dependent and spin-independent part separately, which are given by the $M^2(\langle \mathbf{1} \rangle)$ (spin-independent part) and $M^2(\langle \sigma \rangle) + M^2(\Lambda)$ (spin-dependent part) matrix elements square.

The wave functions and energies of the calculated spectrum of ^{208}Pb, up to excitation energies of the order of 30 MeV, have been included in the calculation of the matrix element $\mathcal{M}(q, q', l\gamma J)$ of Eqs. (14), (18), and (22). They contribute to the noncoherent process and their values, which only depend on the details of the nuclear structure model and are shown in Table II.

In order to evaluate the effects on the matrix elements due to the degree of accuracy in the description of the muon wave functions we have calculated the matrix elements $\mathcal{M}(q, q', l\gamma J)$ by replacing in the radial integral the muon wave function $g(r)$ by its value at the nuclear surface $g(R)$, with R the nuclear radius. The results are shown in Table III.

From the comparison of the results of Tables II and III we may conclude that the proper treatment of the muon wave function amounts to sizable changes in the values of the participant nuclear matrix elements.

TABLE V. Coefficients $C_V(q)$ and $C_A(q)$ $q = p, n$ for the two models for muon conversion in nuclei.

Model	$C_V(p)$	$C_V(n)$	$C_A(p)$	$C_A(n)$
W exchange	1.917	1.083	−1.017	0.017
SUSY	−0.230	3.230	−4.278	4.278

In Table IV we present the contributions of different terms of the effective LFV Lagrangian to the total squared matrix element of the noncoherent process (second column) and its spin-independent (third column) and spin-dependent (fourth column) parts. The fifth and sixth columns of the table show the percentage of spin-independent and spin-dependent contributions. In the analysis we have removed the contribution of the spurious 1^- state associated to the center of mass excitation [39].

In Fig. 3 we present the contributions to the noncoherent squared matrix elements $\mathcal{M}(q, q', l\gamma J)$ of the S-, V-, A-, and T-type operators. It is seen that the scalar and vector terms produce very similar contributions and the same is valid for the axial-vector and tensor operators.

As a particular example of the use of the matrix elements $\mathcal{M}(q, q', l\gamma J)$ and with the coefficients given in Table V, we have calculated the contributions to the W exchange and SUSY processes. The results are shown in Tables VI and VII and in Fig. 4.

It is seen from the histograms shown in Fig. 4 that for the case of W exchange, the spin-independent nuclear transitions are larger than the spin-dependent ones, while for the SUSY model, the contributions of the spin-dependent multipole excitations are larger than the spin-independent one.

The multipole decompositions of the nuclear matrix elements $\mathcal{M}_{\langle\alpha\rangle}(q, q')(\alpha = 1, \sigma, \Lambda)$ of Eqs. (12), (16), and (20) are shown in Figs. 5, 6, and 7. These values are independent of the LFV model. The larger contributions are those of the spin-independent operators.

TABLE VI. Contribution of W-exchange [13] and SUSY [17] models to the total squared matrix element of the noncoherent process (second column), its spin-independent (third column) Eq. (12) and spin-dependent (fourth column) Eqs. (16) and (20) parts. The fifth and sixth columns show the percentages of spin-independent and spin-dependent terms to the total squared matrix element.

Model	Total	Spin-independent	Spin-dependent	Spin-independent/ total (%)	Spin-dependent/ total(%)
W exchange	3.532	2.691	0.841	76.2	23.8
SUSY	34.331	5.024	29.307	14.6	85.4

TABLE VII. Contributions of various multipoles (J^π) to the total squared matrix element of the noncoherent process (second column), its spin-independent (third column) and spin-dependent (fourth column) contributions for the W-exchange model [13]. In columns 5, 6, and 7 we show the results obtained by using the SUSY model [17].

J^π	W exchange			SUSY		
	Total	Spin independent	Spin dependent	Total	Spin independent	Spin dependent
0^-	0.056	0.000	0.056	2.110	0.000	2.110
0^+	0.636	0.636	0.000	1.087	1.087	0.000
1^-	1.217	1.074	0.143	7.134	2.218	4.916
1^+	0.253	0.000	0.253	8.238	0.000	8.238
2^-	0.166	0.000	0.166	5.809	0.000	5.809
2^+	0.735	0.653	0.082	3.934	1.099	2.835
3^-	0.298	0.279	0.019	1.270	0.504	0.766
3^+	0.090	0.000	0.090	3.364	0.000	3.364
4^-	0.025	0.000	0.025	0.920	0.000	0.920
4^+	0.045	0.042	0.003	0.257	0.103	0.155
5^-	0.005	0.005	2×10^{-4}	0.027	0.013	0.014
5^+	0.004	0.000	0.004	0.181	0.000	0.181

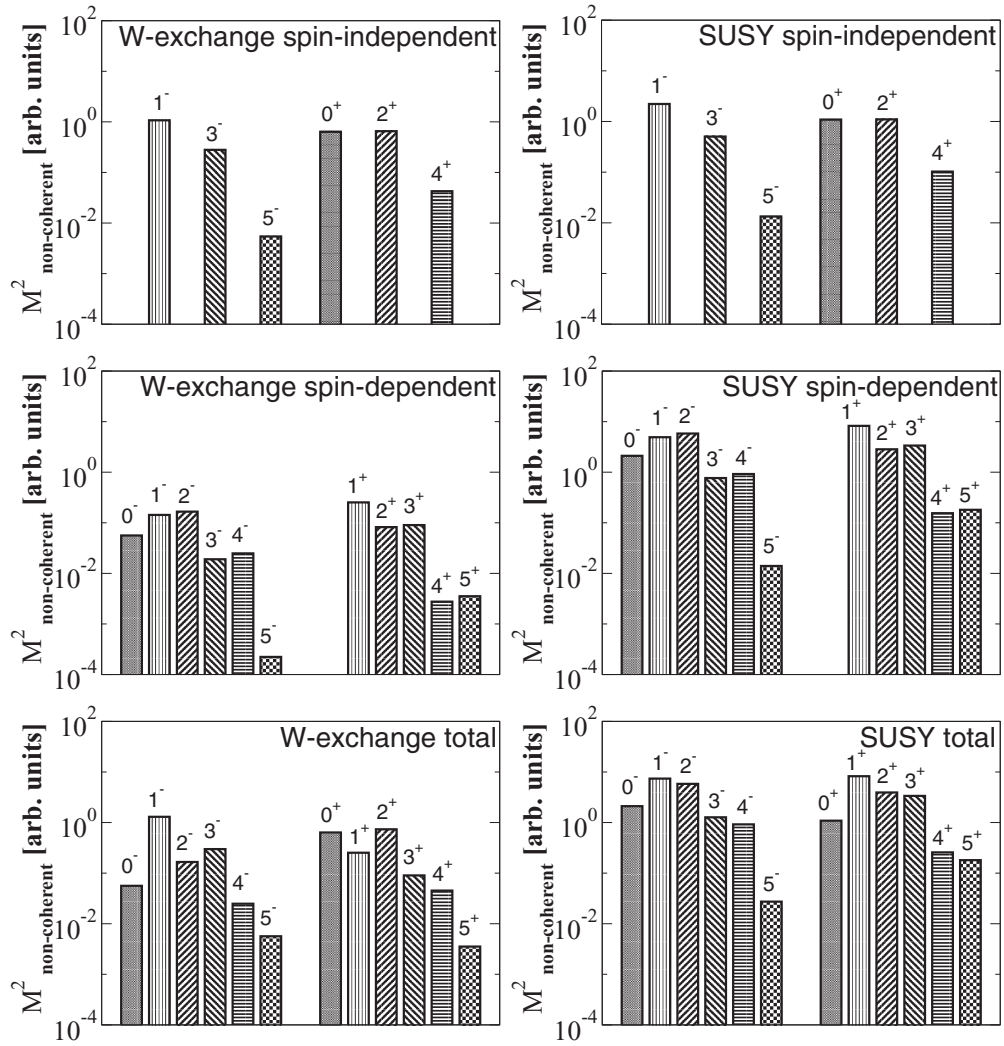

FIG. 4. Multipole decomposition of the squared matrix element of the noncoherent process for two models: W exchange [13] in the left panels, and SUSY [17] in the right panels. The top panels show spin-independent contribution, the middle spin-dependent contributions, and the lowest panels show the total contributions of each multipolarity.

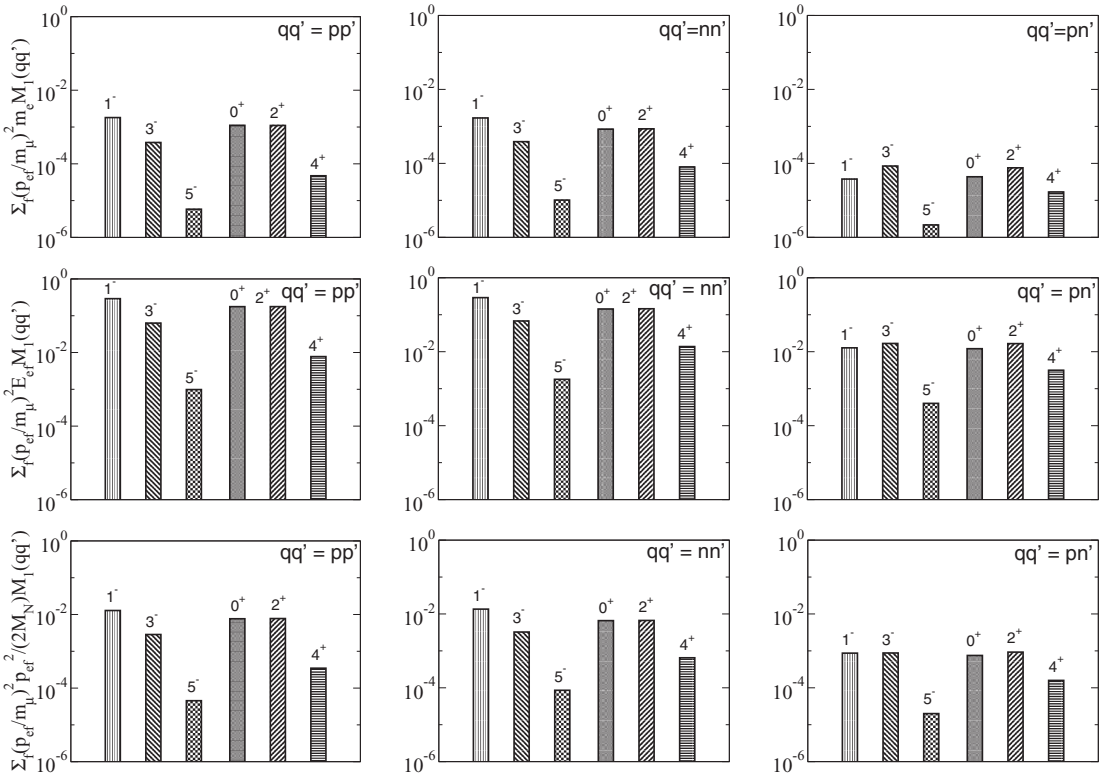

FIG. 5. Multipole decomposition of the squared matrix element of the noncoherent process, for $q, q' =$ proton-particle–proton-hole, neutron-particle–neutron-hole and $q =$ proton-particle–proton-hole, $q =$ neutron-particle–neutron-hole components of the wave function for each multipolarity. The histograms show the contributions to the nuclear matrix elements independently of the LFV model, for the spin-independent channel, $\mathcal{M}_{\langle 1 \rangle}(q, q')$.

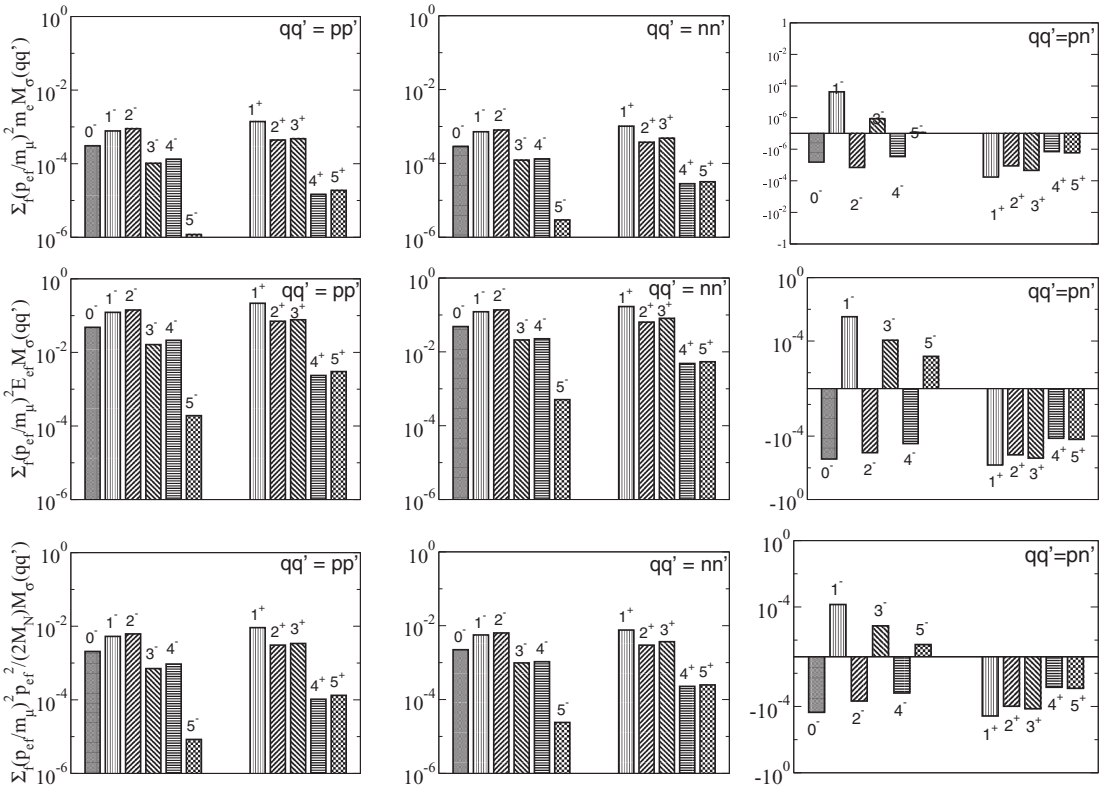

FIG. 6. Same as in Fig. 5 for the spin-dependent nuclear matrix elements $\mathcal{M}_{\langle \sigma \rangle}(q, q')$.

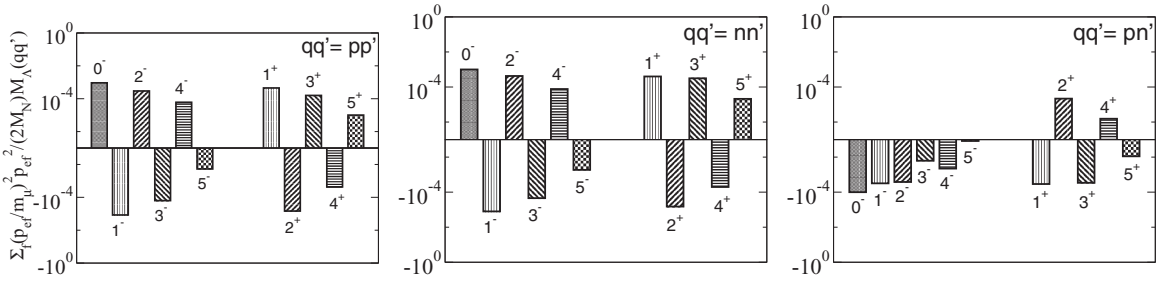

FIG. 7. Same as in Fig. 5 for the spin-dependent nuclear matrix elements $\mathcal{M}_{\langle\Lambda\rangle}(q, q')$.

The form factors of Eqs. (25) are given in Table VIII. The results of the present work, for $A = 208$, are compared with the results obtained in other works, for $A = 27, 48$, and 208 Refs. [11,13] and [19]. Table IX shows the results for the total matrix corresponding to the coherent and noncoherent channels. The quantities given in Table VIII are obtained in the context of the W exchange and SUSY models.

IV. CONCLUSIONS

In this paper we have revisited the case of the muon-to-electron conversion in ^{208}Pb. We have considered here a most general form of the nonphotonic part of the effective four-fermion Lagrangian. To describe the wave functions of the states belonging to the nuclear spectrum we have adopted a δ-force interaction and diagonalized it in the basis of proton (neutron) particle-hole configurations. The nuclear response was then decomposed in multipoles for each of the channels participant accordingly to the structure of the associated operators. This was done in order to facilitate the use of the calculated nuclear matrix elements in modeling LFV processes. The nuclear response was applied to two specific LFV scenarios (W bosons and SUSY particles as mediators). We have discussed the spin dependence of the operators entering the calculated nuclear matrix elements and found that the spin-independent modes yield larger contributions compared to the spin-dependent ones. When using these matrix elements in the W-exchange mechanism the spin-independent modes dominates over the spin-dependent ones, but the situation seems to be the opposite for other LFV modes, like SUSY particle-mediated processes. As expected, and as was found in all previous works, the coherent process is the dominant one since it exhausts practically all of the transition amplitude. However, in view of expected improvements in the sensitivity of future experiments, the estimates of the noncoherent part of the transition amplitude may become of importance.

The theoretical approximations leading to the LFV transition amplitudes are dependent on the assumptions made to approximate the subnucleonic and nucleonic parts of the currents and ultimately on the form of the adopted interactions to describe nuclear correlations, as well as on the specific form of the Lagrangian. While the nuclear part of the calculations may be tested by other means, for instance, by using the same wave functions to calculated electromagnetic transitions, decays, and particle transfer reactions on the nucleus host of the LFV process, the particle-physics part of it is still open to schemes which go beyond the standard model of the electroweak transitions. Then the task to determine the influence of the underlying LFV model in setting up limits on the observability of the $(\mu^- \longrightarrow e^-)$ conversion may be facilitated by the use of the multipole decomposition of the nuclear response as we have done in this work.

TABLE VIII. Proton and neutron nuclear form factors F_Z and F_N calculated in this work using Eq. (25) and results taken from previous works.

Model	A	Z	F_Z	F_N
Ref. [11]	27	13	0.66	0.62
Ref. [19]	27	13	0.667	0.662
Ref. [11]	48	22	0.55	0.52
Ref. [13]	48	22	0.55	0.52
Ref. [11]	208	82	0.25	0.22
This work	208	82	0.28	0.22

ACKNOWLEDGMENTS

This work has been supported by the National Research Council (CONICET) of Argentina (Grants No. PIP 616 and No. PUE-IFLP-2019) and by the Agencia Nacional de Promoción Científica y Tecnológica (ANPCYT) PICT 140492 of Argentina. The authors are members of the scientific research career of the CONICET.

TABLE IX. Square matrix elements for coherent (second column) and noncoherent (third column) transitions for the W-exchange and SUSY models.

Model	$M^2_{\text{gs}\longrightarrow\text{gs}}$	$M^2_{\text{gs}\longrightarrow\text{exc}}$
W exchange	1738.8	3.5
SUSY	2904.3	34.3

[1] Y. Kuno and Y. Okada, Rev. Mod. Phys. **73**, 151 (2001).
[2] L. Calibbi and G. Signorelli, Riv. Nuovo Cimento **41**, 71 (2018).
[3] W. H. Bertl *et al.* (SINDRUM II Collaboration), Eur. Phys. J. C **47**, 337 (2006).
[4] L. Bartoszek *et al.* (Mu2e Collaboration), arXiv:1501.05241.
[5] COMET Collaboration, COMET Phase-I technical design report, http://comet.kek.jp/Documents_files/IPNS-Review-2014.pdf.
[6] S. Weinberg and G. Feinberg, Phys. Rev. Lett. **3**, 111 (1959).
[7] W. J. Marciano and A. I. Sanda, Phys. Rev. Lett. **38**, 1512 (1977).
[8] O. Shanker, Phys. Rev. D **20**, 1608 (1979).
[9] A. Czarnecki, W. J. Marciano, and K. Melnikov, AIP Conf. Proc. **435**, 409 (1998).
[10] T. S. Kosmas and J. D. Vergados, Nucl. Phys. A **510**, 641 (1990).
[11] T. S. Kosmas, G. K. Leontaris, and J. D. Vergados, Prog. Part. Nucl. Phys. **33**, 397 (1994).
[12] H. C. Chiang, E. Oset, T. S. Kosmas, A. Faessler, and J. D. Vergados, Nucl. Phys. A **559**, 526 (1993).
[13] T. S. Kosmas, J. D. Vergados, O. Civitarese, and A. Faessler, Nucl. Phys. A **570**, 637 (1994).
[14] T. S. Kosmas and J. D. Vergados, Phys. Rept. A **264**, 251 (1996).
[15] T. S. Kosmas, J. D. Vergados, and A. Faessler, Phys. Atom. Nucl. **61**, 1161 (1998).
[16] T. S. Kosmas, Z. Ren, and A. Faessler, Nucl. Phys. A **665**, 183 (2000).
[17] T. Siiskonen, J. Suhonen, and T. S. Kosmas, Phys. Rev. C **62**, 035502 (2000).
[18] T. S. Kosmas, S. Kovalenko, and I. Schmidt, Phys. Lett. B **511**, 203 (2001).
[19] J. Kostensalo, J. Suhonen, and O. Civitarese, Phys. Rev. C **98**, 065504 (2018).
[20] R. Kitano, M. Koike, and Y. Okada, Phys. Rev. D **66**, 096002 (2002).
[21] J. Engel, G. C. McLaughlin, and C. Volpe, Phys. Rev. D **67**, 013005 (2003).
[22] C. Volpe, J. Phys. G **30**, L1 (2004).
[23] A. B. Balantekin and G. M. Fuller, J. Phys. G **29**, 2513 (2003).
[24] A. B. Balantekin and H. Yuksel, New J. Phys. **7**, 51 (2005).
[25] O. Civitarese and T. Tarutina, Phys. Rev. C **94**, 054603 (2016).
[26] L. Pescatore, arXiv:1809.06756.
[27] Compilation of muon sources, https://muonsources.org/muon-centres.html.
[28] J. D. Vergados, Phys. Rep. **133**, 1 (1986).
[29] A. Faessler, T. S. Kosmas, S. Kovalenko, and J. D. Vergados, Nucl. Phys. B **587**, 25 (2000).
[30] J. Bernabeu, E. Nardi, and D. Tommasini, Nucl. Phys. B **409**, 69 (1993).
[31] L. L. Foldy and S. A. Wouthuysen, Phys. Rev. **78**, 29 (1950).
[32] M. E. Rose and R. K. Osborn, Phys. Rev. **93**, 1326 (1954).
[33] P. Alexa, J. Kvasil, and R. K. Sheline, Phys. Rev. C **55**, 3170 (1997).
[34] A. Bohr and B. Mottelson, *Nuclear Structure* (Benjamin, Reading, MA, 1969), Vol. 1.
[35] O. Civitarese, R. J. Liotta, and M. E. Mosquera, Phys. Rev. C **78**, 064308 (2008).
[36] I. Hamamoto, Phys. Rep. **10**, 63 (1974).
[37] M. J. Martin, Nucl. Data Sheets **108**, 1583 (2007).
[38] H. de Vries, C. W. de Jager, and C. de Vries, At. Data Nucl. Data Tables **36**, 495 (1987).
[39] D. R. Bes and O. Civitarese, Phys. Rev. C **63**, 044323 (2001).